

## Quantitative study of the interfacial intermixing and segregation effects across the wetting layer of Ga(As,Sb)-capped InAs quantum dots

Esperanza Luna,<sup>1,a)</sup> Ana M. Beltrán,<sup>2,b)</sup> Ana M. Sánchez,<sup>3</sup> and Sergio I. Molina<sup>2</sup>

<sup>1</sup>Paul-Drude-Institut für Festkörperelektronik, Hausvogteiplatz 5-7, D-10117, Berlin, Germany

<sup>2</sup>Departamento de Ciencia de los Materiales e I.M y Q.I., Facultad de Ciencias, Universidad de Cádiz, Campus Río San Pedro, 11510 Puerto Real, Cádiz, Spain

<sup>3</sup>Physics Department, University of Warwick, Coventry CV4 7AL, United Kingdom

(Received 7 March 2012; accepted 13 June 2012; published online 2 July 2012)

Quantitative chemical information from semiconductor nanostructures is of primary importance, in particular at interfaces. Using a combination of analytical transmission electron microscopy techniques, we are able to quantify the interfacial intermixing and surface segregation across the intricate non-common-atom wetting layer (WL) of Ga(As,Sb)-capped InAs quantum dots. We find: (i) the WL-on-GaAs(buffer) interface is abrupt and perfectly defined by sigmoidal functions, in analogy with two-dimensional epitaxial layers, suggesting that the interface formation process is similar in both cases; (ii) indium segregation is the prevailing mechanism (e.g., over antimony segregation), which eventually determines the composition profile across the GaAs(cap)-on-WL interface. © 2012 American Institute of Physics. [<http://dx.doi.org/10.1063/1.4731790>]

Expanding the usable wavelength for opto-electronic devices towards 1.3 and 1.55  $\mu\text{m}$  is a subject of current technological relevance.<sup>1</sup> Present efforts focus on the development of new GaAs-based functional units, where nanostructures based on quantum dots (QDs) remain as one of the most promising options.<sup>2-4</sup> The incorporation of antimony into (In,Ga)As QDs has been found to be an effective solution to redshift the emission, due to the possibility of a staggered type-II band alignment for antimony contents above 14%.<sup>5</sup> Indeed, room temperature emission at 1.6  $\mu\text{m}$  has already been reported with Ga(As,Sb)-capped (In,Ga)As QDs.<sup>6,7</sup> The complexity of the growth of InAs-GaAs-GaSb heterostructures is well-known, in particular, the difficulty of fabricating abrupt heterointerfaces, since both cation and anion segregation may occur.<sup>8,9</sup> Segregation may not only result in the degradation of the interface but also in the unintentional formation of a ternary and/or quaternary alloy from the nominally deposited binary compounds. In addition to the inherent difficulties present in the chemical analysis of any quaternary compound, In and Sb segregation may simultaneously occur, which hampers the detection and evaluation of the individual contributions.<sup>9</sup> The impact of segregation on the structural properties of Ga(As,Sb)-capped InAs/GaAs dot-in-well structures has been studied on the atomic scale by cross-sectional scanning tunneling microscopy.<sup>9,10</sup> While most of the studies focus on the structural and chemical properties of QDs, quantitative analysis of the chemical profile and compositional sharpness of wetting layers (WLs) are scarcely reported. Moreover, recently, intriguing photoluminescence (PL) emission from recombination at the WL interface of In(As,Sb) QDs has been reported.<sup>11</sup> In their work, the authors explicitly demand the need for specific investigations into the structure and composition of the WL interface to fur-

ther understand the WL-related PL feature. Based on the analysis of the intensity contrast of  $g_{002}$  dark-field transmission electron microscopy (DFTEM) micrographs, Luna and co-workers have recently proposed a method for the quantitative evaluation of the chemical intermixing at the interfaces of InAs/GaSb superlattices, which includes segregation effects.<sup>12</sup> The procedure, however, has not yet been applied to the analysis of the chemical interface in nanostructures, e.g., across QDs *per se* or across WLs. In this work, we apply our quantitative DFTEM (qDFTEM) method to the chemical characterization of the interface in a Sb-based non-common-atom (NCA) WL. In particular, we are able to determine the chemical composition, including the identification and quantification of III- and V-element segregation effects, across the interfaces of the intricate (In,Ga)(As,Sb) WL of Ga(As,Sb)-capped InAs QDs grown on GaAs(001).

The studied sample was grown by molecular beam epitaxy and consists of 2.2 monolayers (ML) InAs QDs, capped with 6 ML GaAs and 3 ML GaSb, upon which a 100 nm GaAs cap layer was deposited. The nominal structure is shown in Figure 1(b). Growth conditions can be found elsewhere.<sup>13</sup> The morphological and chemical characterization has been conducted by conventional TEM (CTEM) in cross-sectional view in a JEOL-JEM 1200EX operated at 120 kV.<sup>14</sup> TEM specimens have been prepared following standard procedures. In addition to CTEM, analytical TEM techniques such as electron energy loss spectroscopy (EELS) has been performed.<sup>14</sup> Because we deal with NCA interfaces between quaternary and/or ternary alloys, the unambiguous determination of the WL composition requires the combined analysis of EELS, high-angle annular dark-field scanning transmission electron microscopy (HAADF-STEM), and DFTEM data.

Figure 1(a) shows a cross-sectional  $g_{002}$  DFTEM image of the WL. As already reported in Ref. 12, qDFTEM analysis of the chemical interface in NCA heterostructures relies on the analysis of two-beam DFTEM images obtained with the diffraction vector  $\mathbf{g} = 002$ , which is sensitive to the chemical composition for semiconductors with zincblende structure.

<sup>a)</sup> Author to whom correspondence should be addressed. Electronic mail: luna@pdi-berlin.de. Telephone: +49 30 20377 281. Fax: +49 30 20377 515.

<sup>b)</sup> Present address: n-Mat Group, CEMES-CNRS, 29 Rue Jeanne Marvig, BP 94347, 31055 Toulouse, CEDEX 4, France.

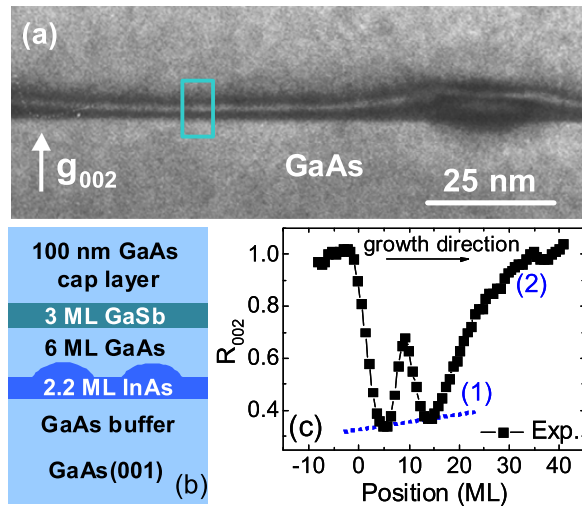


FIG. 1. (a)  $g_{002}$  DFTEM micrograph (sensitive to composition) of the QD structure (b) (not scaled). Also displayed is the area across the WL from where the intensity profile ( $R_{002}$ ) is extracted (c). The labels (1) and (2) in (c) refer to the baseline and to the trail edge at the GaAs(cap)-on-WL interface, respectively.

In short, the method is based on the proposal of a distribution profile for the different constituent elements that we put into the calculation of the corresponding diffracted intensity under kinematic conditions ( $I_{002}$ ). We compare the simulated intensity ( $R_{002}^{\text{sim}}$ ), normalized to that of a reference area of known composition,  $R_{002} = I_{002}^{\text{layer}}/I_{002}^{\text{reference}}$ , with the experimental one ( $R_{002}^{\text{exp}}$ ) and look for the composition profiles best fitting the experimental contrast. Thereby, the procedure would resemble the analysis of x-ray diffraction data where the layer information (composition, thickness, strain, etc.) is extracted after comparing the experimental and simulated curves. Since the identity of cation and anion both change across the heterointerface, we have to input the contributions of the III- and V-sublattices separately, which, in principle, allows the independent determination of the chemical width and surface segregation in each sublattice. Although the method is based on an aperture-limited imaging mode (i.e., DFTEM, with a resolution of about 0.5 nm), the procedure allows the detection of variations in the interface width and layer thickness as small as 0.1 ML.<sup>12</sup> The key issue is the identification of the element distribution profile. Previously, from the analysis of *directly determined* experimental composition profiles in several III-V semiconductor heterostructures, we have demonstrated that the smooth variation of the element concentration  $x(z)$  with the position  $z$  across the interface follows a sigmoidal function:  $x(z) = x_0/[1 + \exp(-z/L)]$ , where the interface width  $L$  is the main fitting parameter and  $x_0$  denotes the nominal mole fraction.<sup>15,16</sup> For layers and/or quantum wells (QWs) centered at  $z = 0$ , the expression reads<sup>15</sup>

$$x = \frac{x_0^{(l)}}{1 + e^{L_{\text{lower}} \left( -\frac{z-N}{2} \right)}} \quad \text{for } z < 0 \quad (\text{lower interface}),$$

$$x = x_0^{(u)} - \frac{x_0^{(u)}}{1 + e^{L_{\text{upper}} \left( -\frac{z-N}{2} \right)}} \quad \text{for } z > 0 \quad (\text{upper interface}).$$

$x_0^{(l)}$  and  $x_0^{(u)}$  denote the nominal mole fraction corresponding to the lower ( $l$ ) and upper ( $u$ ) interface, respectively.  $N$  is the width of the layer, and  $L_{\text{lower}}$  and  $L_{\text{upper}}$  are the interface width at the lower and upper interfaces, respectively. For the analysis of Sb-based NCA interfaces, the realistic distributions for the different elements, In and Sb (those for Ga and As are obtained after mass conservation:  $[\text{In}] + [\text{Ga}] = 100\%$  and  $[\text{As}] + [\text{Sb}] = 100\%$ ) are obtained assuming that the change in composition across the interfaces follows the sigmoidal function in Eq. (1). In order to estimate the presence of segregation effects, we consider input distribution profiles that are obtained from the combination of a segregated profile derived after Muraki's phenomenological model<sup>17</sup> and the sigmoidal function for the description of the interface.<sup>15,18</sup> This innovative procedure has proven very successful in the analysis of InAs/GaSb short-period-superlattices and Sb-based heterostructures, even if extremely thin layers (<3 ML) or (un)intentionally inserted interfacial layers are considered.<sup>12,19</sup>

Figure 1(c) shows the profile of the experimental diffracted intensity normalized to that of GaAs in the buffer layer (reference),  $R_{002} = I_{002}^{\text{layer}}/I_{002}^{\text{GaAs}}$ . The data are extracted from line scans in the area marked in Fig. 1(a), far away from any QD. As observed, the intensity profile reveals a pronounced asymmetry, which resembles segregation features. A previous morphological and *qualitative* chemical characterization of the sample has already revealed that capping the InAs QDs with 6 ML GaAs/3 ML GaSb generates a complex WL consisting of a (In,Ga)(As,Sb) core with Sb-depleted (In,Ga)As interfaces.<sup>14,20</sup> The composition profiles of Figs. 2(a) and 2(c) (open symbols), which are extracted from Ref. 14 and are determined using EELS data (note that EELS investigation for this sample only gives qualitative information<sup>14</sup>) indicate that the In content across the WL is not homogeneous, but there are two indium-rich regions close to the interfaces, which are separated by a thin Sb-containing layer with a reduced In content, i.e., the (In,Ga)(As,Sb) core.

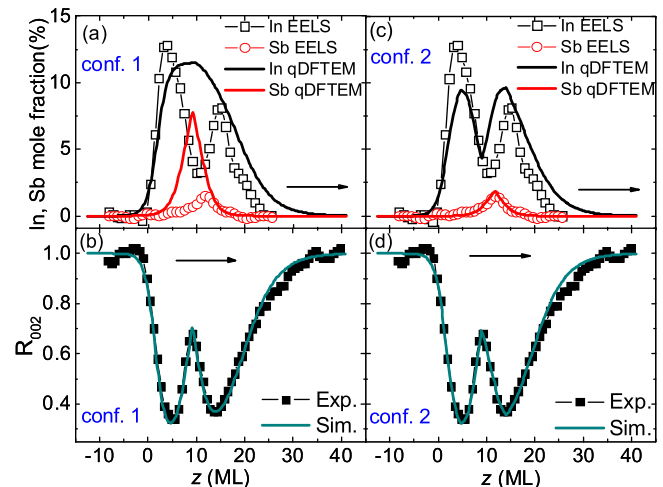


FIG. 2. (a) and (c) Two sets of proposed In and Sb sigmoidal profiles for qDFTEM (solid lines) yielding a similar  $R_{002}^{\text{sim}}$  profile reproducing the experimental intensity ratio,  $R_{002}^{\text{exp}}$  [(b) and (d), respectively]. Segregation effects are not included yet. The growth direction is from left to right (indicated by an arrow).

Despite the comprehensive investigation in Ref. 14, quantitative information on the chemical profile and compositional sharpness of the WL is still missing. In order to quantify the WL interface, we apply the qDFTEM procedure described above, where the first step is the proposal of the input element profiles. Initial fit attempts using element distributions, which are based on the nominal structure (i.e., 2.2 ML InAs/6 ML GaAs/3 ML GaSb) failed, as we found that  $R_{002}^{\text{sim}}$  totally disagreed with  $R_{002}^{\text{exp}}$  (not shown). Next attempts using composition profiles deduced from the EELS data<sup>14</sup> were more successful, as shown in Fig. 2(d), which displays the experimental and simulated intensity profile, together with the corresponding element distribution for qDFTEM along the growth direction (solid lines in Fig. 2(c)). For simplification, segregation effects are not included yet. The In distribution consists of two overlapped peaks (hereafter denoted as In1-peak and In2-peak, respectively), while there is a single Sb profile. The following values for the composition, layer thickness, and interface width are deduced from the fit: 9.9% In,  $N=5.8$  ML and  $L_{\text{lower}}=1.1$  ML,  $L_{\text{upper}}=0.85$  ML for the In1-peak; 11.5% In,  $N=7$  ML and  $L_{\text{lower}}=0.8$  ML,  $L_{\text{upper}}=3.6$  ML for the In2-peak; and 3% Sb,  $N=1.6$  ML and  $L_{\text{lower}}=L_{\text{upper}}=1.5$  ML for the Sb peak. The elemental concentrations are similar to those estimated by EELS.<sup>14</sup> We find, however, that contrary to our previous work on qDFTEM of binary and/or ternary alloys with NCA interfaces,<sup>12,19</sup> where the element profiles could be unambiguously determined, here the set of distribution profiles giving the best fit is not unique, since different combinations of In and Sb distributions can lead to similar results. This arises from the fact that different combinations of In and Sb contents yield similar values of the structure factor and, thus, a similar intensity contrast. Indeed, this is one of the main inherent difficulties associated with the chemical analysis of interfaces between quaternary and/or ternary alloys. We find, for instance, that the set of element profiles in Fig. 2(a), which consists of a single In peak (which could be considered as the envelope of the two In peaks) and a single Sb peak, yields likewise a good fit [except at the upper GaAs(cap)-on-WL interface, Fig. 2(b)] and is very similar to the fit in Fig. 2(d). We denote the profiles in Fig. 2(a) configuration 1 (conf. 1), since there is a single In peak. In a similar way, the profiles shown in Fig. 2(c), consisting of two In peaks, are denoted configuration 2 (conf. 2). The parameters of the fit for conf. 1 are: 12%,  $N=16.2$  ML and  $L_{\text{lower}}=1.1$  ML,  $L_{\text{upper}}=3.6$  ML for the In; and 10.9%,  $N=2.8$  ML and  $L_{\text{lower}}=L_{\text{upper}}=1.5$  ML for the Sb. Other configurations (combinations of In and Sb profiles) can result in similar fits as well. These, however, either involve unrealistic In and/or Sb profiles or are in clear disagreement with the HAADF-STEM and EELS measurements<sup>14,20</sup> and, hence, are not considered. Comparison of the profiles constituting conf. 1 and conf. 2, respectively, provides the following information: (i) although segregation effects are not yet explicitly included, for both configurations, the large broadening at the GaAs-on-WL interface in the In profile ( $L_{\text{upper}}=3.6$  ML) reflects the existence of In segregation at least; (ii) while the element concentrations in conf. 1 are in close agreement with the nominal values (note however that only a small amount of Sb incorporates,

with [Sb] < 11% or, 0.4 ML if computed as the equivalent thickness of GaSb deposited<sup>21</sup>), the In and Sb distributions disagree with the qualitative chemical information extracted from HAADF-STEM and EELS,<sup>14,20</sup> (iii) the composition profiles of conf. 2 agree remarkably well with the profiles extracted from EELS and may explain the peculiar HAADF-STEM contrast at the WL of this sample, as reported in Refs. 14 and 20. The estimate equivalent thickness of InAs at the WL (area under the [In] curve) is close to 1.7 ML, in good agreement with the amount of In deposited before the two-(2D) to three-dimensional (3D) transition occurs.<sup>21</sup> Hence, in the following, we focus on conf. 2. Notice that, due to the complexity of the WL in this specific case, the combined analysis of HAADF-STEM, EELS, and qDFTEM is crucial for the unambiguous determination of the composition across the interface. The intricate WL element distribution may probably arise from a partial capping of the QDs, where the In from the still exposed regions of the QDs will migrate away to form a “new” WL on top of the “nominal” one.<sup>22,23</sup>

Segregation effects can be easily incorporated into the analysis through the input distribution profiles,<sup>12</sup> where the profiles are obtained from a combination of Muraki’s model and the sigmoidal function for the interface description.<sup>15</sup> Again, because of the many parameters involved, the fitting turns out ambiguous and cumbersome in comparison with that on NCA interfaces between binary and/or ternary alloys. The main difficulties arise from: (a) as already mentioned, different combinations of [In] and [Sb] yield similar values of  $R_{002}$ ; and (b) the small amount of Sb into the lattice (<5% for conf. 2) makes detection of Sb segregation challenging. According to (a), we find that the slight baseline in  $R_{002}^{\text{exp}}$  [marked as (1) in Fig. 1(c)] could be explained by both In and Sb segregation, whereas it is hard to distinguish each individual contribution, since they overlap. On the contrary, there are some other specific segregation features, like the trail edge at the upper GaAs-on-WL interface [marked as (2) in Fig. 1(c)], which can only be explained assuming In segregation: Sb segregation mainly affects the baseline on  $R_{002}$  but is not accountable for the strong asymmetry at the GaAs-on-WL interface. Although it is difficult to identify the contribution from Sb segregation, estimate of the Sb segregation efficiency,  $R_{\text{Sb}}$ , indicates a substantial Sb segregation with  $R_{\text{Sb}} > 0.8$ . This would explain the small amount of Sb, which is incorporated into the layer, despite the nominal composition is GaSb. Coexistence of Sb and In segregation is likely.<sup>9</sup> Contrary to the Sb case, the identification of In segregation is feasible. Indeed, the impact of In segregation on the main features of  $R_{002}$  is significant, as it mainly reflects at the trail edge, thus allowing an accurate determination of the In segregation efficiency,  $R_{\text{In}}$ . In this respect, Fig. 3(a) represents the In and Sb profiles based on the element distribution of conf. 2, but now including In segregation, yielding the best  $R_{002}$  fit [Fig. 3(b)]. For simplification, Sb segregation is not explicitly included. As observed, the agreement between the experimental and simulated  $R_{002}$  is excellent. The estimated  $R_{\text{In}}=0.84 \pm 0.01$  is in good agreement with reported  $R_{\text{In}}$  values for In segregation in (In,Ga)As WLs grown at similar conditions.<sup>24,25</sup> From the profiles in Fig. 3(a), two main conclusions can be drawn: (1) as a consequence of In segregation, the GaAs-on-WL interface is very



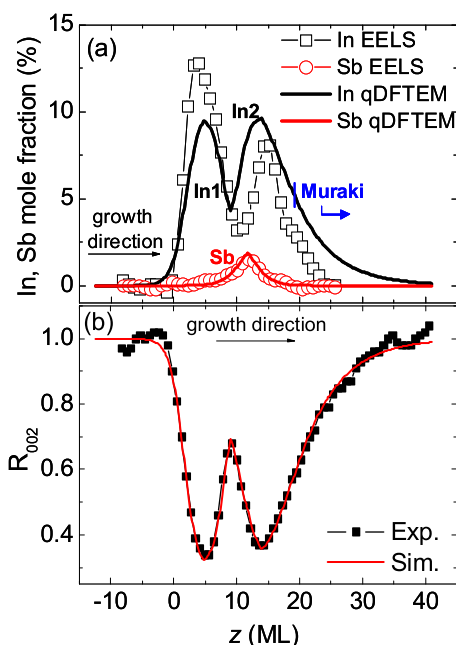


FIG. 3. (a) In and Sb profiles (solid lines) including In segregation at the GaAs-on-WL interface yielding the  $R_{002}^{\text{sim}}$  curve best reproducing the experimental intensity ratio,  $R_{002}^{\text{exp}}$  (b). In segregation efficiency amounts to  $R_{\text{In}} = 0.84$ .

broad and extends over more than 15 ML (4.5 nm) along the growth direction. Thus, In segregation is remarkable and is the prevailing mechanism (e.g., over Sb segregation), which eventually determines the composition profile across the GaAs-on-WL interface. (2) The WL-on-GaAs interface is abrupt and perfectly defined by sigmoidal functions, in analogy with 2D epitaxial layers.<sup>12,15,16</sup> For layers grown in the 2D mode, the sigmoidal response arises from a cooperative incorporation of the species during the interface formation.<sup>26</sup> Hence, we can assume that the processes prevailing in the initial stages of the WL formation are similar to those governing the interface formation in *Frank van der Merwe* 2D layers. How these unexpected results reconcile with the *Stranski-Krastanow* growth mode is presently under investigation.

In summary, using a combination of TEM analytical techniques with qDFTEM, we have quantified the chemical composition and interfacial intermixing (including the identification and quantification of III- and V-element segregation effects) across the complex WL of Ga(As,Sb)-capped InAs QDs. The quantitative analysis of the compositional abruptness in a WL may provide an insight into the basic mechanisms occurring during its formation, further allowing a better understanding and control of the fabrication of functional units based on nanostructures. Moreover, correlations between the optical and chemical properties of WL interfaces can also be established.

We acknowledge J. M. Ripalda and A. G. Taboada from IMM-CSIC (Spain) for the sample growth and M. H. Gass from SuperSTEM Laboratory (U.K.) for the EELS and HAADF data acquisition. DFTEM measurements were

carried out at DME-SCCYT, UCA (Spain). We acknowledge X. Kong and R. Gargallo-Caballero (PDI) for a critical reading of the manuscript. This work was supported by the Spanish MCI (Projects TEC2008-06756-C03-02/TEC and TEC2011-29120-C05-03) and the Junta de Andalucía (PAI research group TEP120; Project P08-TEP-03516). Co-financing from UE-FEDER is also acknowledged. A. M. Sánchez thanks the Science City Research Alliance and the HEFCE Strategic Development Fund for funding support.

- <sup>1</sup>M. Henini and M. Bugajski, *Microelectron. J.* **36**, 950 (2005).
- <sup>2</sup>L. Seravalli, G. Trevisi, P. Frigeri, D. Rivas, G. Muñoz-Matutano, I. Suárez, B. Alén, J. Canet-Ferrer, and J. P. Martínez-Pastor, *Appl. Phys. Lett.* **98**, 173112 (2011).
- <sup>3</sup>D. Alonso-Álvarez, B. Alén, J. M. Ripalda, J. M. Llorens, A. G. Taboada, F. Briones, M. A. Roldán, J. Hernández-Saz, D. Hernández-Maldonado, M. Herrera, and S. I. Molina, *Appl. Phys. Lett.* **98**, 173106 (2011).
- <sup>4</sup>T. V. Hakkarainen, J. Tommila, A. Schramm, A. Tukiainen, R. Ahorinta, M. Dumitrescu, and M. Guina, *Appl. Phys. Lett.* **97**, 173107 (2010).
- <sup>5</sup>H. Y. Liu, M. J. Steer, T. J. Badcock, D. J. Mowbray, M. S. Skolnick, P. Navaretti, K. M. Groom, M. Hopkinson, and R. A. Hogg, *Appl. Phys. Lett.* **86**, 143108 (2005).
- <sup>6</sup>J. M. Ripalda, D. Granados, Y. González, A. M. Sánchez, S. I. Molina, and J. M. García, *Appl. Phys. Lett.* **87**, 202108 (2005).
- <sup>7</sup>H. Y. Liu, M. J. Steer, T. J. Badcock, D. J. Mowbray, M. S. Skolnick, F. Suarez, J. S. Ng, M. Hopkinson, and J. P. R. David, *J. Appl. Phys.* **99**, 046104 (2006).
- <sup>8</sup>J. M. Moison, F. Houzay, F. Barthe, J. M. Gérard, B. Jusserand, J. Massies, and F. S. Turco-Sandhoff, *J. Cryst. Growth* **111**, 141 (1991).
- <sup>9</sup>V. Haxha, I. Drouzas, J. M. Ulloa, M. Bozkurt, P. M. Koenraad, D. J. Mowbray, H. Y. Liu, M. J. Steer, M. Hopkinson, and M. A. Migliorato, *Phys. Rev. B* **80**, 165334 (2009).
- <sup>10</sup>J. M. Ulloa, I. W. D. Drouzas, P. M. Koenraad, D. J. Mowbray, M. J. Steer, H. Y. Liu, and M. Hopkinson, *Appl. Phys. Lett.* **90**, 213105 (2007).
- <sup>11</sup>Y. I. Mazur, V. G. Dorogan, G. J. Salamo, G. G. Tarasov, B. L. Liang, C. J. Rayner, K. Nunna, and D. L. Huffaker, *Appl. Phys. Lett.* **100**, 033102 (2012).
- <sup>12</sup>E. Luna, B. Satpati, J. B. Rodriguez, A. N. Baranov, E. Tournié, and A. Trampert, *Appl. Phys. Lett.* **96**, 021904 (2010).
- <sup>13</sup>J. M. Ripalda, D. Alonso-Álvarez, B. Alén, A. G. Taboada, J. M. García, Y. González, and L. González, *Appl. Phys. Lett.* **91**, 012111 (2007).
- <sup>14</sup>A. M. Sanchez, A. M. Beltran, R. Beanland, T. Ben, M. H. Gass, F. de la Peña, M. Walls, A. G. Taboada, J. M. Ripalda, and S. I. Molina, *Nanotechnology* **21**, 145606 (2010).
- <sup>15</sup>E. Luna, F. Ishikawa, P. D. Batista, and A. Trampert, *Appl. Phys. Lett.* **92**, 141913 (2008).
- <sup>16</sup>E. Luna, F. Ishikawa, B. Satpati, J. B. Rodriguez, E. Tournié, and A. Trampert, *J. Cryst. Growth* **311**, 1739 (2009).
- <sup>17</sup>K. Muraki, S. Fukatsu, Y. Shiraki, and R. Ito, *Appl. Phys. Lett.* **61**, 557 (1992).
- <sup>18</sup>The profiles predicted by the segregation models are based on the assumption of initial perfectly square-like interfaces, which are unlikely to exist in reality.
- <sup>19</sup>T. Taliércio, A. Gassenq, E. Luna, A. Trampert, and E. Tournié, *Appl. Phys. Lett.* **96**, 062109 (2010).
- <sup>20</sup>A. M. Beltran, Ph.D. dissertation, Efecto de la incorporación de antimonio sobre la nanoestructura de puntos cuánticos III-V/III-V, Universidad de Cádiz, Spain, 2009.
- <sup>21</sup>A. Lemaître, G. Patriarche, and F. Glas, *Appl. Phys. Lett.* **85**, 3717 (2004).
- <sup>22</sup>Z. R. Wasilewski, S. Fafard, and J. P. McCaffrey, *J. Cryst. Growth* **201/202**, 1131 (1999).
- <sup>23</sup>A. Lenz, H. Eisele, R. Timm, S. K. Becker, R. L. Sellin, U. W. Pohl, D. Bimberg, and M. Dähne, *Appl. Phys. Lett.* **85**, 3848 (2004).
- <sup>24</sup>P. Offermans, P. M. Koenraad, R. Nötzel, J. H. Wolter, and K. Pierz, *Appl. Phys. Lett.* **87**, 111903 (2005).
- <sup>25</sup>A. Rosenauer, W. Oberst, D. Litvinov, D. Gerthsen, A. Förster, and R. Schmidt, *Phys. Rev. B* **61**, 8276 (2000).
- <sup>26</sup>E. Luna, R. Hey, and A. Trampert, *J. Vac. Sci. Technol. B* **30**(2), 02B108 (2012).